Journal of Physics: Conference Series **2957** (2025) 012001 doi:10.1088/1742-6596/2957/1/012001

Neutrino masses in left-right asymmetric model

Bhabana Kumar and Mrinal Kumar Das

Department of Physics, Tezpur University, Tezpur-784028, India

E-mail: bhabana12@tezu.ernet.in and mkdas@tezu.ernet.in

Abstract. This work presents a comprehensive investigation into the construction of a neutrino mass model utilizing the $\Gamma(3)$ modular group, which exhibits an isomorphism with the A_4 symmetric group. The study focuses on developing a left-right asymmetric model by incorporating modular symmetry. An advantageous aspect of employing modular symmetry in the present model is the elimination of need for additional particles known as "flavons" to break the flavor symmetry. To effectively implement the extended inverse seesaw mechanism, we have introduced one fermion singlet for each generation.

1. Introduction

The standard model (SM) of particle physics is one of the renowned and successful theory, capable of explaining the interactions and properties of fundamental particles. However, despite its remarkable achievements, SM still has some limitations. One of the main drawbacks of SM lies in it's inability to account for the tiny masses of neutrinos due to the absence of right handed neutrino. In the past two decades, scientists have made remarkable progress in the field of particle physics, and the discovery of neutrino oscillation was one of the groundbreaking achievement. The first compelling evidence for neutrino oscillation came in 1998 using the Superkamiokande experiment[1] in Japan, and neutrino oscillation was confirmed by SNO experiment[2, 3]. These discoveries point towards the existence of neutrinos with small and non-degenerate masses. Numerous experiments have been conducted since then in an effort to gain a deeper and better understanding of neutrino masses and mixing. Experiments like MINOS[4], Daya-Bay[5], TK2[6], and RENO[7] have significantly contributed to the growing body of evidence supporting the existence of non-zero neutrino masses. Over the time, our understanding towards the mysteries of neutrino has become more refined, particularly concerning the atmospheric ($\sin^2\theta_{23}$), solar ($\sin^2\theta_{12}$), and reactor ($\sin^2\theta_{13}$) mixing angle. Even though several solar, reactor, and atmospheric experiments have yielded valuable insights into neutrino oscillation parameters(Table 1), there remains a great deal of unanswered questions regarding neutrinos. The recent data from Planck experiments has suggested that 0.11 eV [8, 9], is an approximated upper bound on the sum of the neutrino mass but the precise mass of neutrinos and their hierarchical arrangments continue to pose an intriguing puzzle. Furthermore, the fundamental nature of neutrinos, whether they exhibit Dirac or Majorana properties, remains a subject of ongoing study.

In addition to the neutrino masses, SM also fails to explain several other phenomena. These include the baryon asymmetry of the universe(BAU), which is the observed imbalance between matter and antimatter, the CP violation in weak interactions, and the existence of dark matter.

Table 1. 3σ values of oscillation parameter.

oscillation parameter	for NH	for IH
$\sin^2\theta_{12}$	$0.270 \to 0.341$	$0.270 \to 0.341$
$\sin^2\theta_{23}$	$0.408 \to 0.603$	$0.412 \to 0.613$
$\sin^2\theta_{13}$	$0.02052 \to 0.02398$	$0.02048 \to 0.02416$
$\frac{\Delta m^2_{21}}{10^{-5}}$	$6.82 \to 8.03$	$6.82 \to 8.03$
$\frac{\Delta m^2_{3l}}{10^{-3}}$	$+2.427 \to 2.590$	$-2.570 \to -2.406$

To overcome these limitations of the SM, it is necessary to explore fields beyond the SM. One straightforward approach is to extend the SM by adding new particles. A popular extension of the SM is the see-saw mechanism, which provides a framework for explaining the tiny but non-zero neutrino masses by introducing new scalar or fermion fields.There are several types of see-saw mechanism, including Type I[10], Type II[11], and Type III[12], and inverse-seesaw [13, 14].

Left right symmetric model(LRSM) [15, 16] is an extension of SM where the SM is extended by introducing a new gauge group $SU(2)_R$. The LRSM gauge group is represented by $G_{3221D}(SU(3)_C \times SU(2)_L \times SU(2)_R \times U(1)_{B-L} \times D)$. Where D is the discrete parity symmetry, which connects the $SU(2)_L$ gauge group with the $SU(2)_R$ gauge group and responsible for interchanging the parity of fermion as well as the Higgs field. Non-zero neutrino masses and other drawbacks of SM can be easily explained by using the framework of LRSM. In LRSM both D-parity and $SU(2)_R$ gauge group decoupled spontaneously at the same energy scale and due to that reason we observe equal gauge coupling values for the gauge group $SU(2)_L$ and $SU(2)_R$, i.e., $g_l = g_r$. However, in our present work, we have decided to work in an alternative approach to the LRSM, instead of breaking D parity and $SU(2)_R$ at the same energy scale, this alternative framework focused on breaking the D-parity at some higher energy scale and to break D-parity we need a scalar field σ but it will leave the original gauge group intact. Due to this, we observed unequal gauge coupling values for the gauge group $SU(2)_L$ and $SU(2)_R$ and the result is an asymmetric LRSM [17, 18, 19, 20]. This approach is also an interesting framework to explore because those unequal gauge coupling values can significantly affect various phenomena and can offer novel predictions.

In this work we have used $\Gamma(3)$ modular group of weight two to realized the asymmetric LRSM. The use of modular symmetry in our model has provided a basis in which we can break the flavor symmetry without using any "flavon", instead the modulus τ is in control of breaking the flavor symmetry in our model[21].

The overall structure of the paper is organized as follows: In Section 2, we provide a detailed discussion of the model and derive the mass matrices. Section 3 focuses on our findings and numerical analysis. Finally, we conclude with our results in Section 4.

2. The Model

We have developed a model that incorporates the gauge group G_{2113} $(SU(2)_L \times U(1)_R \times U(1)_{B-L} \times SU(3)_C)$, utilizing the $\Gamma(3)$ modular group and this modular group is isomorphic to A_4 symmetry. We have implemented the extended inverse see-saw mechanism to generate

neutrino masses by adding one sterile fermion (S) per generation. Additionally, the Higgs part of the model is also extended by adding scalar doublet($\chi_{L,R}$) to provide neutrino-sterile (N-S) mixing[22, 23]. The Lagrangian for the neutral fermion, which maintains invariance under the gauge group G_{2113}, is provided below[24].

$$\mathcal{L}' = Y\overline{L}\Psi_R\Phi + f\Psi_R^c\Psi_R\Delta_R + F\overline{\Psi}_R S\chi_R + S^T\mu_s S + h.c \tag{1}$$

The spontaneous symmetry breaking of the Lagrangian, as given in Equation (1), results in a 9×9 mass matrix for the neutral fermions.

$$M = \begin{pmatrix} 0 & 0 & M_D \\ 0 & \nu_S & M \\ M_D^T & M^T & M_R \end{pmatrix}. \tag{2}$$

After complete block diagonalization of the matrix given in equation(2), we obtain the mass matrices for active, sterile, and heavy RH neutrino as follows

$$\begin{aligned} m_\nu &= M_D M^{-1}\mu_S (M_D M^{-1})^T \\ m_S &= \mu_S - M M_R^{-1} M^T \\ m_R &= M_R\ . \end{aligned} \tag{3}$$

In this model, we have incorporated A_4 symmetry by assigning the lepton doublets to transform as triplets under the A_4 group. The RH charged lepton is assigned the transformation (1,1″,1′), also A_4 triplet transformation is attributed to the singlet fermion and the RH neutrino. Furthermore, the scalar sector of the model is assigned a trivial singlet transformation under the A_4 group, implying that it remains invariant under A_4 transformations. To maintain the consistency of the model, we have assigned a distinct charge and modular weight to the particle contents. The charge assignment and modular weight for each particle are provided in Table2.

Table 2. Charges assigned for the particles within the model.

Field	L	Ψ_R	e_R	S	Φ	Δ_R	χ_R	Y
A_4	3	3	1, 1″,1′	3	1	1	1	3
k_I	0	0	0	0	-2	-2	0	2

We have constructed the Lagrangian for the model, keeping in mind that each term of the Lagrangian needs to be invariant under the A_4 symmetry group. The model's Lagrangian is provided in the equation (4).

$$\mathcal{L} = \mathcal{L}_C + \mathcal{L}_N \tag{4}$$

Where $\mathcal{L}_C$ and $\mathcal{L}_N$ is the Yukawa Lagrangian term for the charge and neutral lepton respectively.

The Lagrangian for the charged lepton, which is invariant under A_4 group is given bellow

$$\mathcal{L}_C = \alpha\overline{e}_R\Phi(YL)_1 + \beta\overline{e}_R\Phi(YL)_{1'} + \gamma\overline{e}_R\Phi(YL)_{1''}. \tag{5}$$

Equation (6) represents the mass matrix for the charged lepton that we have constructed using the A_4 symmetry group's multiplication rules

$$M_l = v \begin{pmatrix} \alpha & 0 & 0 \\ 0 & \beta & 0 \\ 0 & 0 & \gamma \end{pmatrix}. \tag{6}$$

Where v represents the VEV of ϕ which is equal to 126 GeV. In this case, the Yukawa term (Y_1,Y_2,Y_3) is assumed to be (1,0,0), allowing us to derive a diagonal mass matrix for the charged lepton. To obtain the desired charged lepton masses, we can adjust the values of α, β, and γ.

The Lagrangian for the neutral lepton sector is given by

$$\mathcal{L}_N = \mathcal{L}_D + \mathcal{L}_R + \mathcal{L}_{N-S} + \mathcal{L}_S \tag{7}$$

where $\mathcal{L}_D$ is the Dirac and $\mathcal{L}_R$ is the Majorana mass term for neutrino respectively. $\mathcal{L}_{N-S}$ and $\mathcal{L}_S$ are the $N-S$ and $S-S$ mixing mass respectively. Since the $\mathcal{L}_D$ can be symmetric as well as asymmetric, we have written A_4 invariant Dirac mass term in the following way

$$\mathcal{L}_D = q_1 \Psi_R \Phi (Y\overline{L})_{3_S} + q_2 \Psi_R \Phi (Y\overline{L})_{3_A}. \tag{8}$$

Where the first term represents the symmetric and the second term represents the asymmetric part of $\mathcal{L}_D$.

$$\mathcal{L}_{N-S} = f_1 \overline{\Psi}_R \chi (YS)_{3_S} + f_2 \overline{\Psi}_R \chi (YS)_{3_A}. \tag{9}$$

By utilizing A_4 group's multiplication rule, we have built, the Dirac, Majorana ,$N-S$ and $S-S$ mixing mass matrices of the model which are given in the equation (10) to (13), respectively.

$$M_D = v \begin{pmatrix} 2q_1Y_1 & (-q_1+q_2)Y_3 & (-q_1-q_2)Y_2 \\ (-q_1-q_2)Y_3 & 2q_1Y_2 & (-q_1+q_2)Y_1 \\ (-q_1+q_2)Y_2 & (-q_1-q_2)Y_1 & 2q_1Y_3 \end{pmatrix} \tag{10}$$

$$M_R = v_R \begin{pmatrix} 2Y_1 & -Y_3 & Y_2 \\ -Y_3 & 2Y_2 & -Y_1 \\ -Y_2 & -Y_1 & 2Y_3 \end{pmatrix} \tag{11}$$

$$M = \chi_R \begin{pmatrix} 2f_1Y_1 & (-f_1+f_2)Y_3 & (-f_1-f_2)Y_2 \\ (-f_1-f_2)Y_3 & 2f_1Y_2 & (-f_1+f_2)Y_1 \\ (-f_1+f_2)Y_2 & (-f_1-f_2)Y_1 & 2f_1Y_3 \end{pmatrix} \tag{12}$$

$$M_S = \mu_S \begin{pmatrix} 1 & 0 & 0 \\ 0 & 0 & 1 \\ 0 & 1 & 0 \end{pmatrix}. \tag{13}$$

Where v_R and χ_R represent the corresponding VEVs of the scalar triplet Δ_R and scalar doublet χ_R. The Majorana mass term associated with the singlet fermion S is represented by M_S. We have also included certain adjustable parameters (q_1, q_2, f_1, and f_2) in our model to obtain the necessary Dirac and $N-S$ mixing mass matrix.

3. Results and Numerical Analysis

The results and findings of the study have been thoroughly discussed and analyzed in this section. To obtain the desired result we have considered the free parameter in the following way.

Real and imaginary value of q_1, $q_2 \in [10^{-5},10^{-3}]$ and for f_1, $f_2 \in [10^{-4},10^{-3}]$.

$v_R \in [1, 100]$ TeV, $\mu_s \in [10, 50]$ keV and $\chi_R \in [1, 100]$ TeV

We have utilized $\Gamma(3)$ modular group within our framework, yielding three modular forms in all and the three Yukawa couplings are represented by these modular forms. In Figures 1 and 2 we can see that the calculated values fall within the range of 10^{-4} to 10. The calculated values of Yukawa couplings are given in the Table 3

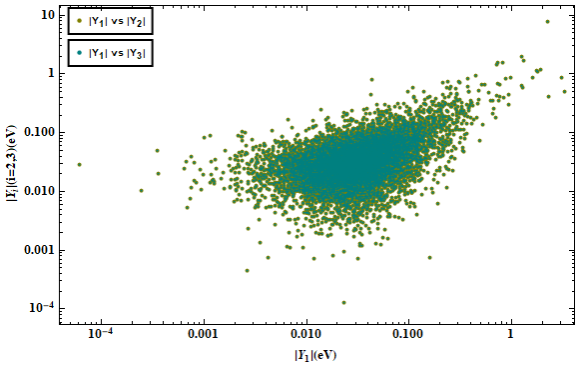

Figure 1. Correlation among Yukawa couplings for NH.

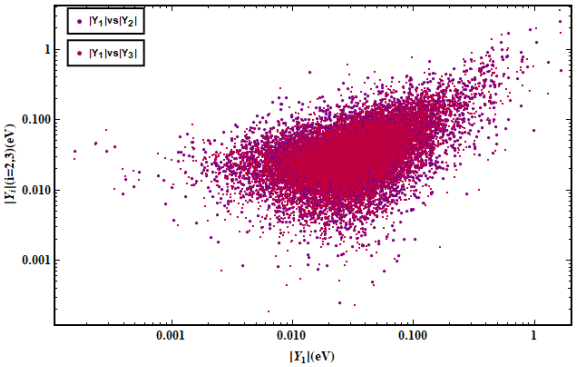

Figure 2. Correlation among Yukawa couplings for IH.

Table 3. Yukawa coupling values for NH and IH.

Yukawa coupling	for NH	for IH
Y_1	$0.61 \times 10^{-4} - 3.25$	$1.64 \times 10^{-4} - 3.26$
Y_2	$0.13 \times 10^{-3} - 7.84$	$0.84 \times 10^{-4} - 2.23$
Y_3	$0.35 \times 10^{-3} - 3.46$	$1.94 \times 10^{-4} - 1.99$

3.1. Active neutrino masses

Figures 3 and 4 depict the relationship between the sum of the neutrino masses ($\sum m_\nu$) and the lightest neutrino mass (m_i where $i = 1$ and 3) for NH and IH respectively. The upper limit on the $\sum m_\nu$, also referred to as the Planck bound, is represented by the horizontal line in Figures 3 and 4. We have found that while a considerable portion of calculated values fall below this bound, some calculated values of the $\sum m_\nu$ exceed it. Furthermore, upon analyzing Figures 5 and 6, we have observed that when the Yukawa coupling values are between 10^{-2} and 10^{-1}, some calculated $\sum m_\nu$ go beyond the allowed limit. However, for all other values of Yukawa coupling, the calculated values of the $\sum m_\nu$ remain well below the experimental bound.

This strange observation suggests that within the specified range of Yukawa coupling values, the calculated values for the $\sum m_\nu$ tend to adhere to the experimental constraints.

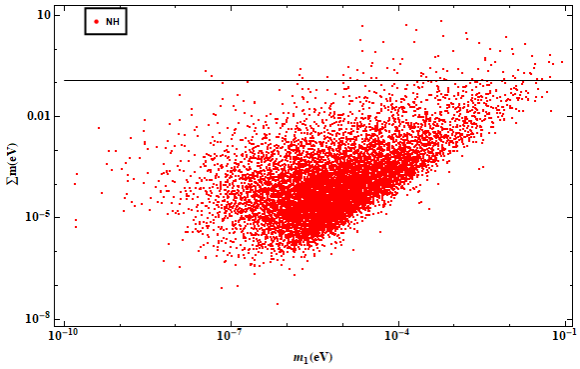

Figure 3. Parameter space for $\sum m_\nu$ and m_1

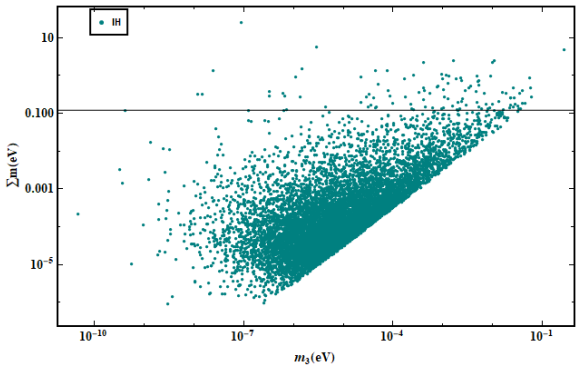

Figure 4. Parameter space for $\sum m_\nu$ and m_3.

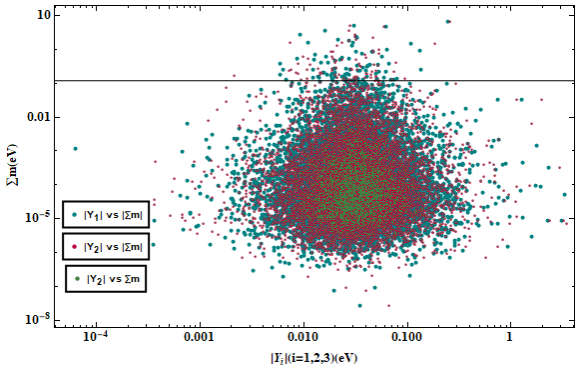

Figure 5. Dependence of $\sum m_\nu$ on (Y_1, Y_2, Y_3) in the NH

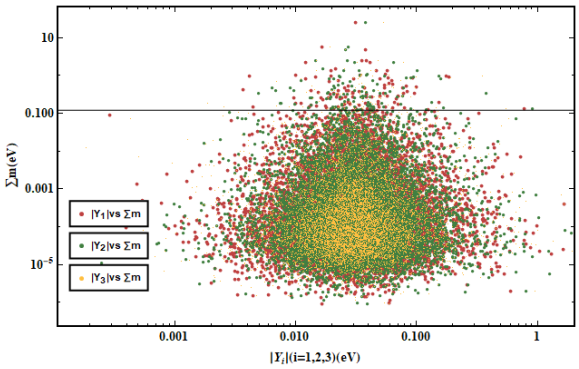

Figure 6. Dependence of $\sum m_\nu$ on (Y_1, Y_2, Y_3) in the IH.

3.2. Right handed neutrino mass

Figures 7 and 8 illustrate the correlation among the RH neutrino masses. They show the relationship of M_{N_1} with M_{N_2} and M_{N_3} for both the hierarchy. The plot of M_{N_1} versus M_{N_2} shows a linear relationship, whereas the plot of M_{N_1} versus M_{N_3} deviates from linearity. After thoroughly analyzing these plots, we concluded that the RH neutrino mass M_{N_1} is the heaviest among the three RH neutrinos, M_{N_3} is the lightest, and they satisfy the condition $M_{N_1} \approx M_{N_2} > M_{N_3}$.

3.3. Sterile fermion mass

To observe the correlation among the sterile fermion masses, we conducted a similar analysis to the one performed for right-handed neutrinos. In Figure 9, we noted that both plots—showing the variation of M_{S_1} against M_{S_2} and M_{S_1} against M_{S_3} exhibited a scattered pattern. From this observation, we concluded that the sterile fermion mass M_{S_1} is greater than or equal to M_{S_2}, and the sterile fermion mass M_{S_3} is the smallest among them. Similar plots were observed for the IH, leading us to conclude that the sterile fermion masses follow the relation $M_{S_1} \geq M_{S_2} > M_{S_3}$, which holds for both the NH and IH cases.

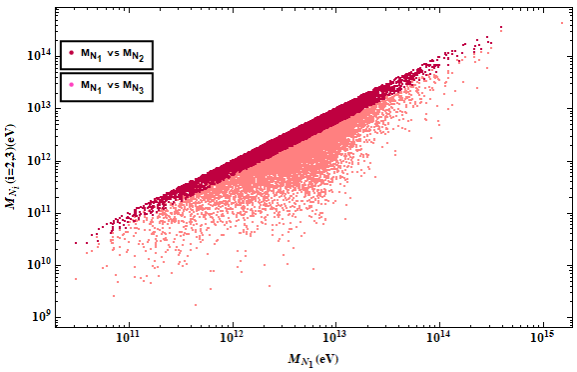

Figure 7. Relationship between RH neutrino masses in the NH.

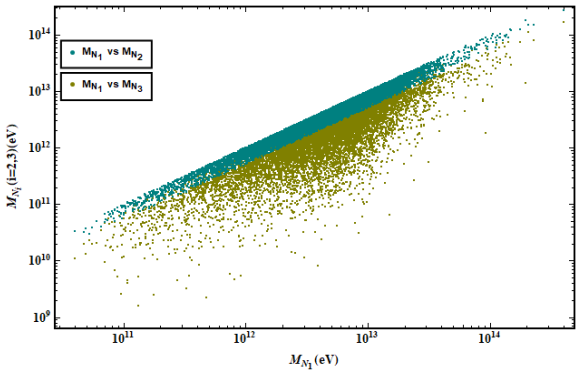

Figure 8. Relationship between RH neutrino masses in IH.

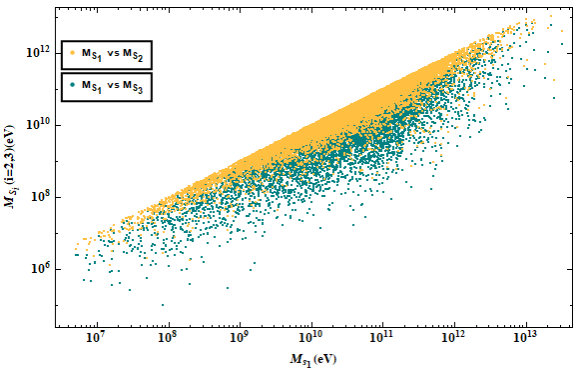

Figure 9. Relationship between sterile fermion masses in the NH.

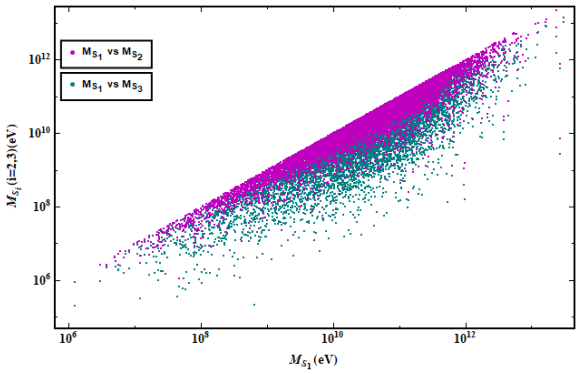

Figure 10. Relationship between sterile fermion masses in the IH.

4. Conclusion

In this study, we have investigated the asymmetric LRSM utilizing the gauge group G_{2113} and incorporating the $\Gamma(3)$ modular group of weight 2. One of the main advantages of this model is the absence of flavon fields due to the use of modular group. The three Yukawa couplings of the model are expressed in terms of the modulus τ and it is found that the absolute value of modulus τ lies within the range of 0.0085 to 5.91. By employing the extended inverse seesaw mechanism, we have successfully generated the light neutrino mass. To accomplish this, we introduced one sterile fermion per generation. Some of the calculated $\sum m_\nu$ exceeds the Planck bound but we have noted that only a few data points lie above the bound, while the majority still remain well below it. Furthermore, we have examined the Yukawa coupling values (Y_1,Y_2,Y_3) and found that they range from 0.884×10^{-4} to 3.26. In Figures 5 and 6, we observed that within the range of Yukawa coupling from 10^{-2} to 10^{-1}, a few of the calculated values of the $\sum m_\nu$ exceed the Planck bound. Therefore, we can conclude that, except for this range, all other values of Yukawa coupling yield suitable results for the calculation of neutrino masses. This does not mean that the Yukawa values within this range produce no results at all; rather, they do not yield results as suitable as those obtained from other Yukawa coupling values. Lastly, we have investigated the mass hierarchy of the heavy RH neutrinos and sterile fermions. We have found that the RH neutrinos follow the mass hierarchy $M_{N_1} \approx M_{N_2} > M_{N_3}$, while the sterile fermions exhibit the mass hierarchy $M_{S_1} \geq M_{S_2} > M_{S_3}$.

In LRSM, both gauge couplings are equal, so their ratio does not impact the calculation of the effective mass and half-life of $0\nu\beta\beta$ decay, in the calculation of LFV, or the calculation of the CP asymmetry term, but within our current framework, we have implemented a left-right asymmetric setup characterized by unequal gauge coupling values. So it is possible that these differing gauge couplings can primarily impact phenomena like $0\nu\beta\beta$ decay, LFV, and the calculation of BAU. Overall, our study presents a framework based on the asymmetric LRSM employing modular symmetry. It offers valuable insights into neutrino masses, mixing, and the mass hierarchy of the involved particles.

References

[1] Fukuda Y *et al.* (Super-Kamiokande) 1998 *Phys. Rev. Lett.* **81** 1562–1567
[2] Bandyopadhyay A, Choubey S, Goswami S and Kar K 2001 *Phys. Lett. B* **519** 83–92
[3] Ahmad Q R *et al.* (SNO) 2002 *Phys. Rev. Lett.* **89** 011301
[4] Evans J (MINOS) 2013 *Adv. High Energy Phys.* **2013** 182537
[5] An F P *et al.* (Daya Bay) 2012 *Phys. Rev. Lett.* **108** 171803
[6] Abe K *et al.* (T2K) 2011 *Phys. Rev. Lett.* **107** 041801
[7] Lasserre T, Mention G, Cribier M, Collin A, Durand V, Fischer V, Gaffiot J, Lhuillier D, Letourneau A and Vivier M 2012
[8] Ade P A R *et al.* (Planck) 2014 *Astron. Astrophys.* **571** A16
[9] Aghanim N *et al.* (Planck) 2020 *Astron. Astrophys.* **641** A6 [Erratum: Astron.Astrophys. 652, C4 (2021)]
[10] Schechter J and Valle J W F 1980 *Phys. Rev. D* **22** 2227
[11] Antusch S and King S F 2004 *Phys. Lett. B* **597** 199–207 (*Preprint* `hep-ph/0405093`)
[12] Foot R, Lew H, He X G and Joshi G C 1989 *Z. Phys. C* **44** 441
[13] Deppisch F and Valle J W F 2005 *Phys. Rev. D* **72** 036001
[14] Abada A and Lucente M 2014 *Nucl. Phys. B* **885** 651–678
[15] Mohapatra R N and Pati J C 1975 *Phys. Rev. D* **11** 2558
[16] Bhupal Dev P S, Mohapatra R N, Rodejohann W and Xu X J 2019 *JHEP* **02** 154
[17] Chang D, Mohapatra R N and Parida M K 1984 *Phys. Rev. D* **30** 1052
[18] Borah D, Patra S and Sarkar U 2011 *Phys. Rev. D* **83** 035007
[19] Sruthilaya M, Mohanta R and Patra S 2018 *J. Phys. G* **45** 075004
[20] Chang D, Mohapatra R N and Parida M K 1984 *Phys. Rev. Lett.* **52** 1072
[21] Feruglio F
[22] Awasthi R L, Parida M K and Patra S 2013 *JHEP* **08** 122
[23] Senapati S, Patra S, Pritimita P and Majumdar C 2020 *Nucl. Phys. B* **954** 115000
[24] Hati C, Patra S, Pritimita P and Sarkar U 2018 *Front. in Phys.* **6** 19